J. Phys. D: Appl. Phys. 27 (1994) 2340–2348. Printed in the UK

Low-pressure gas breakdown in combined fields

V A Lisovsky and V D Yegorenkov

Kharkov State University, Svobody 4, Kharkov, 310077, Ukraine

Received 21 June 1993, in final form 27 April 1994

Abstract. This paper reviews measured and theoretical data relating to the low-pressure discharge breakdown in DC and uniform RF fields and their combination. The original results on determination of molecular constants of various gases from breakdown curves obtained by the authors are given. We have investigated the effect of the DC electric field on the RF breakdown pattern. In particular the influence of the DC electric field on the ambiguity region of the RF discharge breakdown curves has been determined. Breakdown equations in combined fields have been derived and comparison has been made between these equations and measured data. Simple analytical criteria for gas breakdown for a wide range of parameters have been given.

1. Introduction

RF capacitively coupled discharges and combined (RF field plus external constant electric field) discharges are widely used in many technological processes [1–11]. To optimize plasma technological processes it is often necessary to know gas breakdown conditions in a discharge device. Therefore it is of considerable interest to simulate and measure the breakdown curves in uniform RF and combined RF and DC fields.

The paper by Kirchner [12] was one of the first remarkable papers devoted to RF gas breakdown. However, the extremely large spread of breakdown voltage values measured by him prevents one from judging the shape of the breakdown curve. Actually, detailed data on breakdown curves of a RF discharge in hydrogen have been measured, for example by Githens [13] and Chenot [14]. Hale [15] suggested a simple model of RF gas breakdown. Pim [16] investigated RF breakdown in air inside a gap of less than 1 mm width between plane parallel electrodes in a frequency range between 100 and 300 MHz.

Kihara [17] performed a mathematical treatment of electric discharges in gases by choosing models simulating processes occurring when electrons collide with gas particles, these models being based on measured data. Assuming the isotropic part of the electron distribution function over velocities to be Maxwellian, Kihara showed that if the electron temperature satisfies a certain equation then the electron distribution function (EDF) satisfies the Boltzmann equation—the right-hand side of which (in the frame of adopted models) accounts for its change due to elastic as well as inelastic collisions. Kihara [17] applied the results obtained, in particular, to the solution of the problem of RF breakdown for a uniform field and diffusion regime. The equation determining the breakdown criterium contained a term accounting of electron losses due to the oscillatory motion of bulk electrons with respect to ions being at rest. This motion of bulk electrons is due to their drift and, as the directed velocity of electrons exceeds their diffusional velocity, the motion occurs in phase with changes in the RF field applied. The possible secondary emission of electrons from the surface of electrodes has not been taken into account. However the RF breakdown equation has not given a satisfactory description of measured data [13]. In trying to improve the agreement between theory [17] and measured data [13], Sen and Ghosh [18] suggested changing the numerical values of the molecular constants used by Kihara [17], determining them not from the models adopted in [17] but from the known measured data. However, this did not give the expected improvement. Anashkin [19] refined the validity region of the diffusion theory applied by Kihara [17] and established the region in the limits of which electron depletion from the discharge gap is determined mainly by the drift pattern of electron motion.

As is known [20, 21] in the region of small pressures there is a region of an ambiguous dependence of RF breakdown voltage U_{RF} on gas pressure p to the left of the minimum of breakdown curves. Such an ambiguity region is present in a RF discharge breakdown not only by increasing the RF voltage but also by decreasing it. On lowering the pressure the RF discharge voltage first decreases, it passes through an inflection point and a minimum, then it grows and approaches the first turning point. The subsequent growth of the RF breakdown voltage occurs with increasing gas pressure, i.e. an ambiguity region is observed on the RF discharge breakdown curve. Leaving the second turning point, the

0022-3727/94/112340+09$19.50

RF discharge breakdown curve deflects to low pressures. In this region, after the breakdown, the RF discharge burns in its strong current form whereas other parts of the breakdown curve are responsible for the weak current form.

At the same time the combined discharge corresponding to the weak current form of the RF discharge is described by the non-monotonic dependence of the RF discharge breakdown voltage U_{RF} on the applied constant voltage U_{DC}. On increasing the constant voltage the RF breakdown voltage first grows [12, 16, 20, 22–24], approaches a maximum and then decreases [16, 20, 25, 26]. With the strong current form of the RF discharge one observes only the monotonic decrease of RF breakdown voltage with the constant voltage growing [16, 20].

Refinement of the agreement between measured data and theoretical predictions may be performed in two ways. One way [27–30]—called microscopic—clarifies the processes of forming distribution functions of particles in a discharge due to collisions. The phenomenological method chosen in this paper has been applied earlier [17] and is convenient for constructing breakdown models using molecular constants and, in particular, for the treatment of technological gases. The phenomenological approach is also based on microscopic processes in the discharge, but it is less rigorous.

This paper studies both experimentally and theoretically the gas breakdown in uniform RF and combined RF and DC fields.

2. Experimental details

The combined discharge was made in air, argon, CF_4 and other gases at low pressures ($p = 10^{-2}$–10 Torr) and the RF frequency $f = 13.56$ MHz. The spacing between plane stainless steel electrodes of 100 mm in diameter was changed in the limits $L = 7$–54 mm. DC voltages were in the limits $U_{DC} = 0$–600 V and RF voltages were $U_{RF} = 0$–1000 V.

The RF and DC voltages were applied to the same electrodes. The RF voltage was fed to one of the electrodes and another electrode was grounded. A choke of 4 mH inductance was connected in parallel to the electrodes, i.e. self-bias was absent. The potential electrode served as an 'anode' (a positive DC potential was applied to it), the grounded electrode played the role of the 'cathode'.

We have not employed an external ionization source in order to study the self-sustained discharge breakdown.

The process of measuring the RF breakdown curves differs from corresponding conventional measurements of the DC discharge. As first pointed out by Levitskii [20], one should make them in a different way in different pressure ranges. In the range of pressures exceeding that corresponding to the minimum RF voltage value, one can employ the conventional technique of fixing the pressure and increasing the voltage until breakdown occurs. In the range of lower pressures, one should fix the voltage and increase the pressure until breakdown occurs.

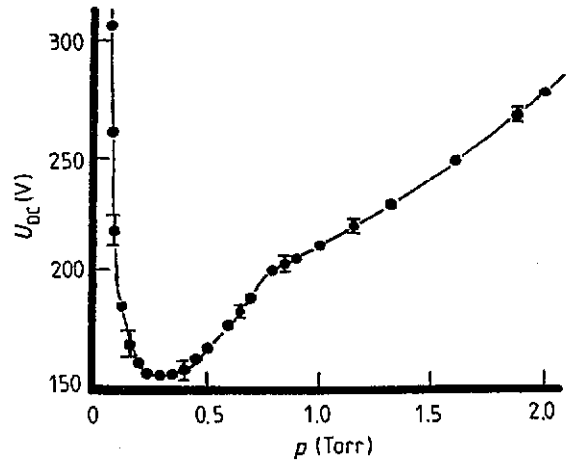

Figure 1. DC breakdown voltage against argon pressure for $L = 23$ mm.

Dealing with the combined discharge, we have acted as follows. At higher pressures we first applied the DC voltage across the discharge gap and then increased the RF voltage across it until breakdown occurred. At lower pressures we applied DC and RF voltages across the gap simultaneously and then increased the pressure until breakdown was achieved.

In all cases the appearance of the active current in the discharge circuit and of light in the discharge chamber served as indicators of breakdown.

The accuracy of the DC breakdown voltage measurements was ±5 V near and to the right of the DC curve minimum and ±10 V to the left of the minimum (figure 1). The accuracy of the RF breakdown voltage measurements U_{RF} was ±2 V in the range $U_{RF} \leqslant 500$ V and ±5 V in the range $U_{RF} > 500$ V. The time lags of the breakdown do not exceed 3–5 s in the total ranges of gas pressures and RF and DC voltages under study. Considerable time lags (1–10 min) were observed only when the electrodes were coated with materials possessing inferior emission properties (e.g. soot [31] or polymer films with complicated surface relief [32]).

3. Gas breakdown in RF and DC electric fields

Let us take the Kihara equation [17] for the RF gas breakdown

$$\exp\frac{B_0 p}{2E} = A_1 pL\left(1 - \frac{E/B_0 p}{C_2 L/\Lambda}\right) \qquad (1)$$

where $E = E_{RF}/\sqrt{2}$ is the effective RF field, p is the gas pressure, L is the electrode spacing. Λ is the vacuum wavelength of the RF field, A_1, B_0, C_2 are the molecular constants [17], and we find the first dU_{RF}/dp and second d^2U_{RF}/dp^2 derivatives. Then for the minimum and inflection points of the RF breakdown curve we obtain the following expressions

$$p_{min} = \frac{1 + (\Lambda/2C_2L)}{A_1 L}\exp\left(1 + \frac{\Lambda}{2C_2 L}\right) \qquad (2)$$

Table 1. Molecular constants A_1, B_0, and C_2.

Gas	A_1 (cm Torr)$^{-1}$		B_0 V cm^{-1} Torr^{-1}				C_2	
	This Paper	[17]	This paper	[17]	[33]	[34]	This paper	[17]
Air	3.0 ± 0.1	—	220 ± 5	—	365	—	3116 ± 25	—
N_2	—	6.5	—	340	342	—	—	660
O_2	3.4	—	185	—	—	—	4016	—
H_2	7.3	2.5	170	130	130	—	1250	560
He	2.8	0.81	75	50	34	—	3100	530
Ne	—	1.53	—	80	100	—	—	730
Ar	9.0	5.2	184	200	180	—	7149	520
CF_4	9.7	—	235	—	—	—	3950	—
CCl_4	19.0	—	615	—	—	—	1500	—
CH_4	—	6.2	—	300	—	192	—	750
C_3F_8	14.0	—	450	—	—	—	2300	—
SF_6	22.0	—	670	—	—	—	3300	—
C_6H_{12}	16.0	—	400	—	—	400	3000	—

$$\left(\frac{U_{RF}}{pL}\right)_{min} = \frac{B_0/\sqrt{2}}{1 + (\Lambda/2C_2L)} \tag{3}$$

$$\left(\frac{U_{RF}}{pL}\right)_{inflection} = \frac{B_0/\sqrt{2}}{2 + (\Lambda/2C_2L)}. \tag{4}$$

It is easy to solve equations (2)–(4) for molecular constants A_1, B_0 and C_2:

$$C_2 = \frac{\Lambda(1 - Z)}{2L(2Z - 1)} \tag{5}$$

$$A_1 = \frac{1 + (\Lambda/2C_2L)}{(pL)_{min}} \exp\left(1 + \frac{\Lambda}{2C_2L}\right) \tag{6}$$

$$B_0 = \sqrt{2}\left(\frac{U_{RF}}{pL}\right)_{min}\left(1 + \frac{\Lambda}{2C_2L}\right) \tag{7}$$

$$B_0 = \sqrt{2}\left(\frac{U_{RF}}{pL}\right)_{inflection}\left(2 + \frac{\Lambda}{2C_2L}\right) \tag{8}$$

where

$$Z = \frac{(U_{RF}/pL)_{inflection}}{(U_{RF}/pL)_{min}} \qquad \tfrac{1}{2} < Z < 1. \tag{9}$$

Table 1 gives the values of molecular constants A_1, B_0 and C_2 for different gases calculated according to equations (5)–(8) from our measured data on RF discharge breakdown curves (see figures 3, 5 and 8 later). The values of molecular constants A_1 and B_0 from table 1 describe well the measured breakdown curves of the RF discharge in the range of interelectrode spacings $L \approx 15$–55 mm. For $L \leqslant 15$ mm the values of A_1 and B_0 depend on L and one should perform additional measurements to clarify this dependence. The results of such studies will be published elsewhere.

The values of the constant B_0 obtained from equations (7) and (8) are close to each other (for air $B_0 = 220 \pm 5$, see figure 3). As is seen from table 1, the measured values of the constant C_2 in this work are larger than those obtained theoretically [17]. Already, Kihara has pointed out the divergence between calculated and measured C_2 values; the reason being that at low gas pressures (near and to the left of the RF discharge breakdown curve minimum) electron emission from electrodes plays an important role in the breakdown—the model in [17] has not included this effect. The influence of surface effects on RF discharge breakdown curves has been studied in detail [31].

The DC breakdown equation is

$$\gamma(e^{\alpha L} - 1) = 1 \tag{10}$$

where α and γ are the first and second Townsend's coefficients. If α is inserted in (10) in the form

$$\alpha = A_0 p \exp\left(-\frac{B_0 pL}{U_{DC}}\right) \tag{11}$$

where A_0 is the molecular constant [17], then for the DC breakdown voltage it is easy to obtain that

$$U_{DC} = \frac{B_0 pL}{\ln(pLA_0/\Gamma)} \tag{12}$$

where $\Gamma = \ln[(1 + \gamma)/\gamma]$. Putting the first and second derivatives of U_{DC} over pL equal to zero we find the expressions for the minimum and inflection points of the DC breakdown curve:

$$\begin{aligned} (pL)_{min} &= \frac{\Gamma}{A_0}e \qquad & U_{DC.min} &= \frac{B_0 T}{A_0}e \\ (pL)_{inflection} &= \frac{\Gamma}{A_0}e^2 \qquad & U_{DC.inflection} &= \frac{B_0\Gamma}{2A_0}e^2 \end{aligned} \tag{13}$$

where e is the base of natural logarithms. Dividing the pressure and voltage at the inflection points by pressure and voltage at the minimum point we can write the following relations

$$\begin{aligned} \frac{U_{DC.inflection}}{U_{DC.min}} &= \frac{e}{2} \\ \frac{p_{inflection}}{p_{min}} &= e. \end{aligned} \tag{14}$$

Kropotov *et al* [21] obtained for the RF breakdown that

$$\frac{U_{\text{RF.inflection}}}{U_{\text{RF. min}}} = \frac{e}{2}$$
$$\frac{e}{2} < \frac{p_{\text{RF.inflection}}}{p_{\text{RF. min}}} < e. \tag{15}$$

Figure 1 shows that for the DC breakdown curve in argon that we have measured

$$\frac{U_{\text{DC.inflection}}}{U_{\text{DC. min}}} \approx 1.31$$
$$\frac{p_{\text{inflection}}}{p_{\text{min}}} \approx 2.67 \tag{16}$$

i.e. the calculated values (14) are supported by measured data satisfactorily.

As is known [35] precise measurement of the location of the breakdown curve minimum makes it possible to calculate the molecular constant B_0 values for any gas under study without knowing the emission properties of the electrode material

$$\left(\frac{U_{\text{DC}}}{pL}\right)_{\text{min}} = B_0. \tag{17}$$

However relations (13) show that one can determine the molecular constant B_0 from measured data on the breakdown curve inflection point

$$\left(\frac{U_{\text{DC}}}{pL}\right)_{\text{inflection}} = \frac{B_0}{2}. \tag{18}$$

The value $(U_{\text{DC}}/pL)_{\text{min}} = (E_{\text{DC}}/p)_{\text{min}}$ at the minimum (17) corresponds to Stoletov's point where the ionization ability of the electron $\eta = \alpha/E_{\text{DC}} = A_0/(B_0 e)$ is maximum [35]. However, at the inflection point (18) the ionization ability of the electron is $1/2e$ less than at the breakdown curve minimum point.

Using equations (17) and (18) as well as DC breakdown curves measured here, we obtain for argon $B_0 = 220 \pm 5$, for air $B_0 = 446 \pm 5$, for CF_4 $B_0 = 728 \pm 5$. Comparison of values obtained from DC breakdown curves with B_0 from table 1 gives that $(B_0)_{\text{DC}} > (B_0)_{\text{RF}}$. The same conclusion may also be drawn from the results of Githens [13] for hydrogen: for E–chamber $(B_0)_{\text{DC}} = 193$, $(B_0)_{\text{RF}} = 144$; for A–chamber $(B_0)_{\text{DC}} = 254$, $(B_0)_{\text{RF}} = 178$. The constant B_0 is the 'effective' ionization potential [35] which includes not only energy losses by electrons due to excitation of electron oscillatory and rotational levels of molecules but also losses of the electrons themselves (e.g. attachment of electrons to molecules). In the DC electric field, an electron, having ionized or excited a certain amount of gas molecules, is lost at the anode due to the drift in the DC electric field. In the RF field electrons are lost at electrodes only from a definite region with the width the $A = KE_{\text{RF}}/\omega$ (K is the electron mobility, $\omega = 2\pi f$) near each of the electrodes. The rest of electrons remain in the interelectrode gap due to oscillations in the RF field. Therefore with RF breakdown electron losses

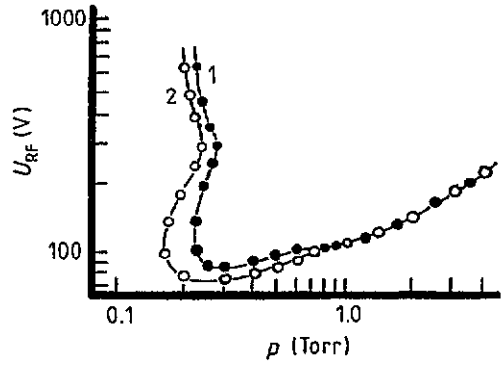

Figure 2. RF breakdown voltage against air pressure for $L = 20$ mm. Curve 1 is for stainless steel electrodes; curve 2 is for duraluminium electrodes [31].

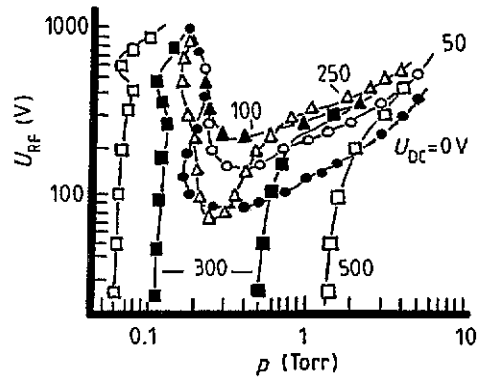

Figure 3. RF breakdown voltage against air pressure for $L = 23$ mm and different DC voltages.

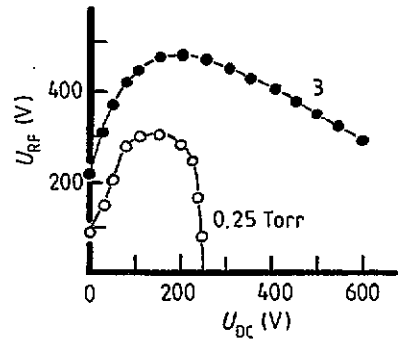

Figure 4. RF breakdown voltage against the DC voltage for $L = 23$ mm and different air pressures.

are remarkably lower. Besides, with DC breakdown, electrons colliding with molecules only lose their energy, whereas with RF breakdown the presence of collisions is one of the conditions for electrons to gain energy [36]. Perhaps this is the reason for $(B_0)_{\text{DC}} > (B_0)_{\text{RF}}$.

The value of the constant A_0 can be determined from equations (12) and (13) only if one knows the ion–electron emission coefficient γ of the electrode material exactly. As we were not in possession of the equipment to measure γ, the constant A_0 has not been measured.

To the right of the inflection point of the DC breakdown curves we measured for air and argon are in good agreement with those from the literature [37].

The appearance of the inflection points at DC breakdown curves has also been observed previously

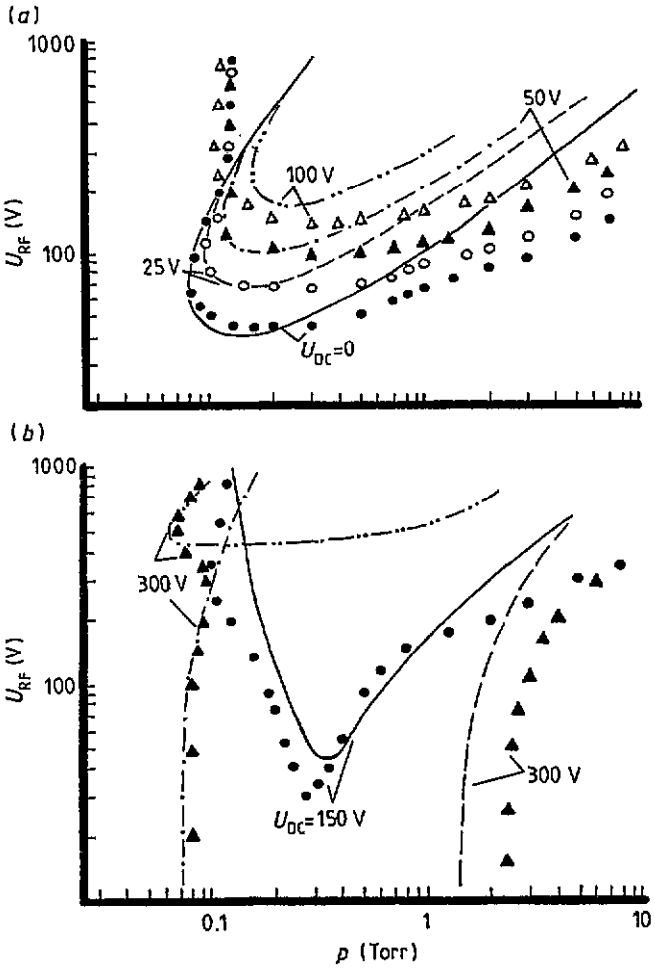

Figure 5. RF breakdown voltage against argon pressure for L = 23 mm and different DC voltages. (*a*) symbols denote measured data and curves give calculated data (calculation from equation (21)): ——, U_{DC} = 0; – – –, 25 V; — · —, 50 V; — · · —, 100 V. (*b*) Symbols denote measured data and curves give calculated data: ——, calculation from equation (26) (U_{DC} = 150 V); – – –, calculation from equation (26), U_{DC} = 300 V; — · —, calculation from equation (27), U_{DC} = 300 V; — · · —, calculation from equation (29), U_{DC} = 300 V.

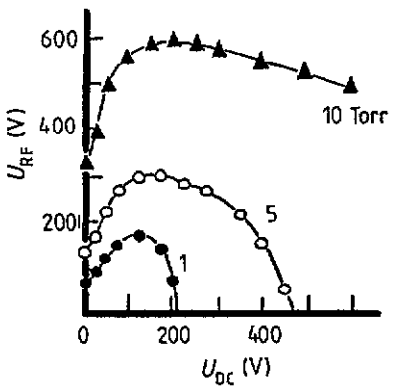

Figure 6. RF breakdown voltage against DC voltage for L = 23 mm and different argon pressures.

[38–40]. Obviously, the inflection point presence in the breakdown curve is theoretically due to the complicated dependence of the first Townsend coefficient on the electric field E. However, the inflection point is also of

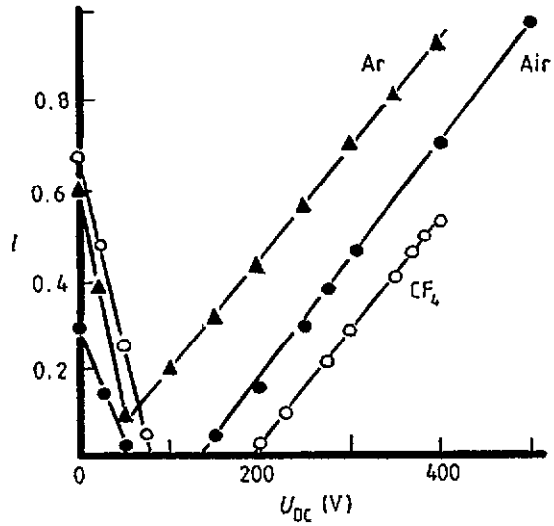

Figure 7. Relative width of the ambiguity region against the DC voltage for air, CF_4 and argon; L = 23 mm.

interest in other ways. RF breakdown curves depend on the electrode material only for pressures $p \lesssim p_{inflection}$ [31] whereas for $p > p_{inflection}$ RF breakdown curves are close for electrodes of various materials (figure 2). In section 4 we show that if RF and DC electric fields are applied simultaneously then the strongest decrease of the breakdown RF voltage at DC voltages close to the discharge DC breakdown potential begins just at the pressure $p \approx p_{inflection}$ (see figures 3, 5(*b*) and 8). From these results one may conclude that surface phenomena (ion–electron and secondary electron emissions) participate at pressures $p < p_{inflection}$; at pressures $p > p_{inflection}$ volume phenomena dominate, i.e. ionization of gas molecules by an electron impact.

4. Gas breakdown in combined fields (experimental)

At the limits of the ambiguity region the RF discharge breakdown curve passes through two turning points. Let us denote the gas pressure at the left boundary of the ambiguity region by p_1, and the respective pressure value at the right boundary by p_2. Let us introduce the relative width of the ambiguity region $l = (p_2 - p_1)/p_1$. The difference of pressures at two turning points is divided by p_1 because, for different electrode spacings L, the ambiguity region may be located in different pressure ranges. For example, for air and L = 7.5 mm the ambiguity region is in the region of 6.4–7 Torr and for L = 23 mm it is in the region of 0.19–0.24 Torr. For CF_4 at $L \lesssim 10$ mm the ambiguity region is not observed; at L = 23 mm it lies in the region of 0.1–0.17 Torr and at L = 29 mm it is in the region of 0.05–0.09 Torr. Therefore it is expedient to choose the quantity $l = (p_2 - p_1)/p_1$ to describe the behaviour of the ambiguity region [26].

It was established in the course of these studies that the small DC voltage induces a noticeable increase of the RF breakdown voltage at the right-hand branch of

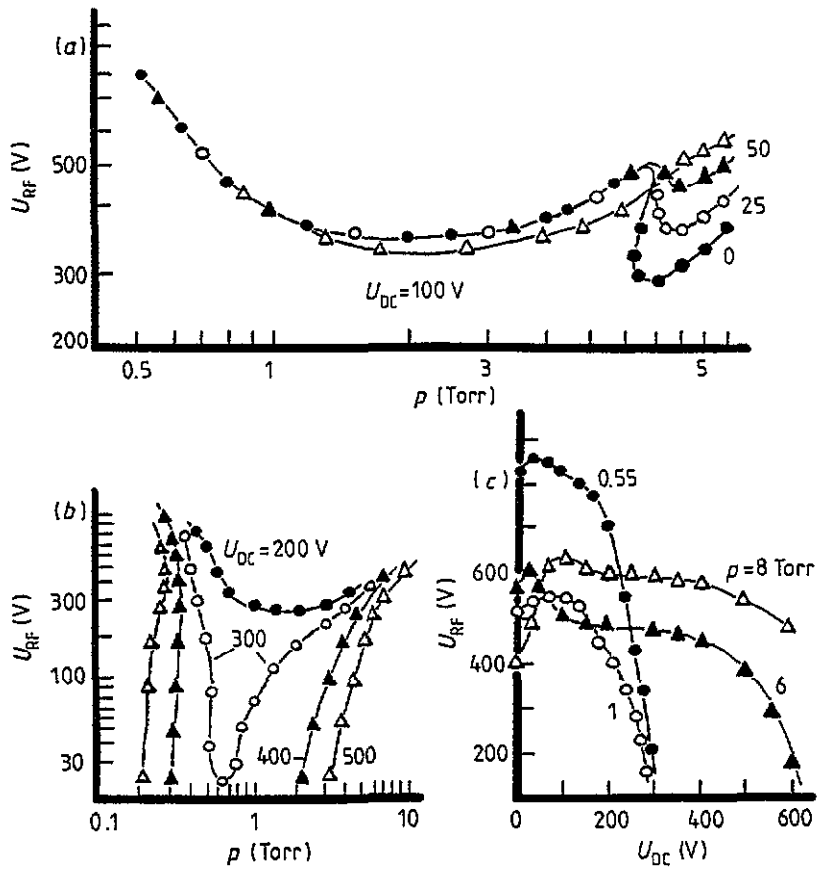

Figure 8. (*a*), (*b*) RF breakdown voltage against air pressure for $L = 7.5$ mm and different DC voltages. (*c*) RF breakdown voltage against DC voltage for $L = 7.5$ mm and different air pressures.

the breakdown curves (figures 3 and 4 give the data for air, and figures 5 and 6 for argon). On increasing the DC voltage the width l decreases approximately linearly (figure 7) and the minimum of the breakdown curve is shifted to higher pressures. At large DC voltages when the DC field contributes to the gas ionization, the RF breakdown voltage approaches the maximum value and then it decreases, approaching zero when the DC voltage becomes equal to the breakdown potential of the DC discharge (figures 4 and 6). The minimum of the breakdown curve shifts to lower pressures and the ambiguity region appears again at the left-hand branch (figures 3 and 5), its width l increasing linearly with growing DC voltage. At large RF voltages the left-hand branches of the breakdown curves of the combined discharge approach asymptotically the RF dicharge breakdown curve without the DC voltage. Figures 3 and 5 show that the appearance of the ambiguity region at large DC voltages is observed at RF voltages exceeding or approximately equal to the DC voltage ($U_{RF} \gtrsim U_{DC}$).

For CF_4 at small DC voltages ($U_{DC} \lesssim 30$ V) the RF breakdown voltage grows considerably slower with the DC voltage increasing than for argon and air and only for higher DC voltage values the RF breakdown voltage grows considerably with the DC voltage increasing. At the same time the ambiguity region is more pronounced in CF_4 at large DC voltages and $U_{RF} \lesssim U_{DC}$ than in air and argon.

For small electrode spacings ($L \leqslant 10$ mm) the ambiguity region is weakly pronounced and to remove it is sufficient to apply DC voltage $U_{DC} \sim 25$ V (figure 8). For small spacings L the second minimum may appear at the RF discharge breakdown curve as has been shown previously [13, 20]. The enhancement of the DC voltage leads to the disappearance of the minimum corresponding to the weak current form of the RF discharge. On the breakdown curves of the combined discharge there remains only the second minimum corresponding to the strong current form of the RF discharge. For small spacings L there is no ambiguity region at large DC voltages U_{DC} and $U_{RF} \geqslant U_{DC}$.

In contrast to the result of Levitskii [20] we obtained that, at the section of the breakdown curve corresponding to the strong current form of the RF discharge (near and to the left of the second minimum in figure 8(*a*)), the increase of the DC voltage at first induces a small growth of the RF breakdown voltage $U_{RF} \sim 5$–30 V (figure 8(*c*)) and only at higher DC voltages does the RF breakdown voltage approach zero. In the region where weak current RF discharge occurs the behaviour of breakdown curves of the combined discharge agrees with that of Levitskii [20]. We have noted a misprint in the caption to figure 6 that work [20]. Instead of $p = 70$ mm Hg one should read $p = 7$ mm Hg. If we take this correction into account, complete agreement between our results and those of Levitskii [20] in the total U_{DC} range is obtained.

Our results also agree qualitatively with those of Pim [16] obtained for higher frequencies and smaller gaps.

5. Gas breakdown in combined fields (theory)

It is difficult to interpret the results obtained for an arbitrary ratio of the RF and DC field amplitudes. Therefore, for simplicity, we consider two limiting cases.

5.1. Weak DC field

Consider first the RF discharge with a small DC electric field applied to it; the DC field does not contribute to gas ionization. Then in the criteria of RF breakdown [17]

$$\frac{L_{RF}^2}{\pi^2}\frac{\nu_i}{D} = 1 \tag{19}$$

where $\Lambda_{RF} = L_{RF}/\pi$ is the diffusional length of the discharge vessel in the presence of a RF field, $L_{RF} = L - (2KE_{RF})/\omega$, E_{RF} is the RF field amplitude, ν_i is the ionization frequency, D is the diffusion coefficient, K is the electron mobility, $\omega = 2\pi f$. Instead of Λ_{RF} the diffusional length of the vessel for the simultaneous action of RF and weak DC electric fields $\Lambda_{DC} = L_{DC}/\pi$ may be used [41,42]:

$$L_{DC} = L_{RF}\left[1 + \left(\frac{E_{DC}L_{RF}}{2\pi D/K}\right)^2\right]^{-1/2} \tag{20}$$

where E_{DC} is the DC electric field value. After changing ν_i, D and K with expressions from [12] we come to the equation governing RF breakdown with a superimposed weak DC electric field:

$$A_1 pL\left(1 - \frac{E/B_0p}{C_2L/\Lambda}\right) = \exp\left(\frac{B_0p}{2E}\right)\left\{1 + \left[\frac{E_{DC}}{E_{RF}}\left(1 - \frac{E/B_0p}{C_2L/\Lambda}\right)A_1pL \times \left(\frac{c_i\rho}{2\sigma}\right)^{1/2}\right]^2\right\}^{1/2} \tag{21}$$

where c_i, ρ and σ are molecular constants tabulated in [17], Λ is the vacuum wavelength of the RF field and $E = E_{RF}/\sqrt{2}$. For $E_{DC} = 0$ we recover from equation (21) the Kihara equation (1). For $p \geqslant p_{inflection}$ and $U_{DC} \geqslant 20$ V

$$D_1 \equiv \left[\frac{E_{DC}}{E_{RF}}\left(1 - \frac{E/B_0p}{C_2L/\Lambda}\right)A_1pL\left(\frac{c_i\rho}{2\sigma}\right)^{1/2}\right]^2 \gg 1. \tag{22}$$

Therefore equation (21) reduces to

$$\exp\left(\frac{B_0p}{2E}\right) = \frac{E_{RF}}{E_{DC}}\left(\frac{2\sigma}{c_i\rho}\right)^{1/2}. \tag{23}$$

For $p_1 \leqslant p \leqslant p_{inflection}$ and $U_{DC} \leqslant 150$ V

$$D_1 \lesssim 1. \tag{24}$$

Kihara [17] obtained the equation (1) for RF breakdown using the drift diffusional approach, i.e. for $\nu_c \gg \omega$ (ν_c is the frequency of collisions between electrons and gas molecules). On deriving the breakdown equation in the combined field we have also employed the drift diffusional approach, therefore the effective RF field is assumed as $E = E_{RF}/\sqrt{2}$ and not $E = \nu_c E_{RF}/[2(\nu_c^2 + \omega^2)]^{1/2}$ as suggested in [41].

In contrast to the breakdown equation obtained in [24], equation (21) permits one to consider the action of the DC field on the ambiguity region. Comparing theoretical and experimental breakdown curves (figure 5(*a*)) one sees that breakdown curves calculated from equation (21) agree satisfactorily with measured breakdown curves in the region where (21) is applicable.

The behaviour of the ambiguity region described above for small DC voltages may be explained as follows. To ignite the discharge it is necessary that the number of charged particles arising as a result of ionization of gas molecules by electron impact be equal to the number of particles leaving the volume because of diffusion and drift in the DC electric field.

First consider the reason for the ambiguity region to appear during the RF breakdown (there is no DC electric field). Let U_1 denote the RF voltage value corresponding to the first turning point of the RF discharge breakdown curve. Let the RF voltage applied across the electrodes exceed U_1 a little but still too low to cause secondary electron emission from the electrodes. Then at the pressure $p = p_1$ breakdown cannot occur because during the half period of the RF field the electrons are displaced at a distance exceeding half the interelectrode spacing and most of the electrons leave the discharge gap without ionizing the number of gas molecules necessary for RF discharge breakdown. For the RF breakdown to occur it is necessary either to apply a sufficiently large RF voltage that would induce secondary electron emission from electrodes or to enhance the pressure, i.e. to supply a large number of gas molecules in the path of exiting electrons. Therefore at $U_{RF} \geqslant U_1$ the breakdown curve moves to the region of larger pressures, i.e. the ambiguity region arises. If the electrons can cross almost all the interelectrode gap during a half period of the RF field, gain a considerable amount of energy and cause secondary electron emission from electrodes, then the breakdown curve of the RF discharge passes through the second turning point and then deflects to the region of lower pressure.

Simultaneous application of a RF and a small DC field induces an enhanced drift of electrons to the electrodes, losses of charged particles increase, therefore the discharge may be ignited only at higher RF voltages and gas pressures (the minimum and turning points of the discharge curve corresponding to the weak current RF discharge are shifted to higher pressures and RF voltages). If the RF voltage and pressure values are such that during a half period of the RF field the electron passes through a distance exceeding half the interelectrode gap and gains (in the combined field) the

energy necessary to give a secondary electron, then the ambiguity region disappears.

At larger DC voltages when the DC field contributes to the ionization of gas molecules by electrons and causes ion–electron emission from the surface of electrodes the discharge may be ignited at lower gas pressures and RF voltages. In this case we go beyond the applicability limits of equation (21).

5.2. Strong DC field

Here we consider the DC voltage to be close to the breakdown potential of the DC discharge, therefore we take equation (10) as the first approximation and instead of the DC field E_{DC} we introduce, according to [41], the effective field E_{eff}

$$E_{eff}^2 = E_{DC}^2 + \frac{\nu_c^2}{\nu_c^2 + \omega^2} \cdot \frac{E_{RF}^2}{2} \tag{25}$$

where ν_c is the rate of electron–atom collisions. Then the following breakdown equation is

$$U_{RF} = \left\{ \frac{2(\nu_c^2 + \omega^2)}{\nu_c^2} \left[\left(\frac{B_0 pL}{\ln(A_0 pL/\Gamma)} \right)^2 - U_{DC}^2 \right] \right\}^{1/2}. \tag{26}$$

As seen in figure 5(*b*) in the applicability region of equation (26), breakdown curves calculated from (26) agree satisfactorily with measured breakdown curves.

At low pressures (to the right of the turning point of the breakdown curve of the RF discharge, $p \leqslant p_1$) the displacement amplitude of electrons in the RF field becomes comparable to the interelectrode spacing. Therefore we account for the effect the RF oscillations of electrons have on the breakdown in the DC field by changing the interelectrode spacing L by L_{RF}. Then the breakdown equation in combined fields assumes the form

$$A_0 pL_{RF} \exp\left(-\frac{B_0 p}{E_{eff}} \right) = \ln \frac{1+\gamma}{\gamma}. \tag{27}$$

For large DC voltages U_{DC}, low pressures and RF voltages $U_{RF} \geqslant U_{DC}$, the measured breakdown curve deflects to the region of lower pressures. Let us try to explain this phenomenon, considering the breakdown evolution at various moments of the RF field period. During the half period of the RF field, when the DC and RF voltages combine, electrons gain energy in the total effective E_{eff} and are lost to the electrode not ionizing a sufficient number of gas molecules to break the discharge. Ions formed due to gas molecule ionization are accelerated in the DC field and collide with electrodes inducing the ion–electron emission. Due to the small rate of ionizing collisions this half period is unfavourable for igniting the discharge. During the other half of the RF field period, when the DC and RF field cancel, electrons gain energy in a comparatively small field E^*

$$E^* = \left(\frac{\nu_c^2}{\nu_c^2 + \omega^2} \cdot \frac{E_{RF}^2}{2} - E_{DC}^2 \right)^{1/2} \tag{28}$$

and they may perform a sufficient number of ionizing collisions to ignite the discharge before they are lost on the electrode. Ion–electron emission from the electrodes is then the additional source of charged particles because inert ions are not subject to the influence of the RF field and they are accelerated only in the DC field. The secondary electron emission may also appear. The breakdown occurs, perhaps, just during this half period of the RF field and it develops as a RF breakdown with the change of the interelectrode spacing L for L_{DC}:

$$A_1 pL_{DC} = \exp\left(\frac{B_0 p}{2E^*} \right). \tag{29}$$

Ion–electron emission helps to ignite the discharge at lower gas pressures. However, the increase of the RF voltage helps the electrons to pass through the interelectrode gap not only during the first but also during the second half period of the RF field. Electron losses on the electrodes grow and the discharge breakdown may now occur only at higher pressures. The breakdown curve passes through the turning point and the ambiguity region appears again at the left-hand branch.

Figure 5(*b*) shows that the measured curve agrees satisfactorily with equations (27) and (29) at RF voltages $U_{RF} < U_{DC}$ and $U_{RF} \geqslant U_{DC}$ respectively.

To conclude this section let us discuss the validity conditions of the drift diffusional approximation in describing the role of the effective RF field in the discharge in combined fields. The possibility of applying the drift diffusional approach to the description of the effective RF field is associated with the magnitude of the DC electric field. This relationship reflects the fact that a weak DC electric field mainly increases the losses of charged particles whereas strong DC fields leads to ionization and an increase in the number of charged particles.

At moderate electrode spacings ($L \lesssim 2.5$ cm) when the breakdown curves of RF and combined discharges lie in the region of sufficiently large gas pressures ($\nu_c \gg \omega$), the drift diffusional approach can be applied and equations (25), (26) and (28) are simplified:

$$E_{eff}^2 = E_{DC}^2 + \frac{E_{RF}^2}{2} \tag{30}$$

$$U_{RF} = \sqrt{2} \left\{ \left(\frac{B_0 pL}{\ln(A_0 pL/\Gamma)} \right)^2 - U_{DC}^2 \right\}^{1/2} \tag{31}$$

$$E^* = \left(\frac{E_{RF}^2}{2} - E_{DC}^2 \right)^{1/2}. \tag{32}$$

However, at larger spacings $L > 2.5$ cm the breakdown curves of the combined discharge lie in the pressure region where $\nu_c \gtrsim \omega$ (especially at large DC voltages U_{DC}) and the drift diffusional approach is not applicable. For example, at $L = 3$ cm the minimum of the RF discharge breakdown curve is attained at pressures $p \approx 0.1$ Torr. For argon $\nu_c \approx 5.3 \times 10^9 p$ s^{-1} Torr^{-1} [33],

therefore at $p = 0.1$ Torr $\nu_c = 5.3 \times 10^8$ s^{-1}. With the RF generator frequency $f = 13.56$ MHz this gives $\nu_c/\omega \approx 6$. But the application of a weak DC voltage U_{DC} shifts the breakdown curve of the combined discharge to the region of higher pressures, the ratio ν_c/ω increases and the drift diffusional approach is quite applicable. At larger DC voltages U_{DC} the breakdown curve of the combined discharge shifts to lower pressures. For example, at $U_{DC} = 600$ V the breakdown curve in argon in the ambiguity region approaches the pressure $p \approx 0.05$ Torr and in CF_4 under similar conditions the pressure is $p \approx 0.03$ Torr. The ratio ν_c/ω becomes of the order of unity, therefore with strong DC electric fields we should use equations (25), (26) and (28) to describe the measured breakdown curves. Returning to the weak DC field case, we note that direct calculations have shown that equation (21) with constants A_1, B_0 and C_2 taken from table 1, describes the measured data satisfactorily not only at moderate L but also at $L \sim 4$–5 cm relating to the region where the drift diffusional approach is no longer applicable. Therefore it was not necessary to derive the gas breakdown equation in combined fields for a weak DC electric field at $\nu_c \approx \omega$.

6. Conclusions

This paper analyses the equations of gas breakdown in RF and DC electric fields. On the grounds of measured breakdown curves for various gases we have obtained the molecular constants used by Kihara in the theory of RF breakdown. We have also studied the influence of the DC electric field on the RF breakdown of the discharge and, in particular, we determine its influence on the size of the region where the RF breakdown voltage depends on pressure ambiguously. The relative width of the ambiguity region l is shown to decrease linearly up to zero on increasing the DC voltage. At large DC voltages, when the DC field contributes to the gas ionization, the ambiguity region appears again at the left-hand branch of the breakdown curve, its width l increasing linearly with increasing DC voltage. We have also derived the breakdown equations for the combined field for different ratios of RF and DC field values. The results of calculations agree satisfactorily with measured data on breakdown curves within the applicability limits of the equations obtained.

References

[1] Flamm D L, Donnelley V M and Ibbotson D E 1983 *J. Vac. Sci. Technol.* B **1** 23
[2] Coburn J 1982 *Plasma Chem. Plasma Process* **2** 1
[3] Ligenza J R 1965 *J. Appl. Phys.* **36** 2703
[4] Miles J L and Smith P H 1963 *J. Electrochem. Soc.* **110** 1240
[5] Kobayashi K, Mutsukura N and Machi Y 1986 *J. Appl. Phys.* **59** 910
[6] Vora H and Moravec T J 1981 *J. Appl. Phys.* **52** 6151
[7] Myshenkov V I and Yatsenko N A 1981 *Kvantovaya Electron. (Quant. Electron.)* **8** 2121 in Russian
[8] Eckbreth A C and Davis J W 1972 *Appl. Phys. Lett.* **21** 25
[9] Brown C O and Davis J W 1972 *Appl. Phys. Lett.* **21** 480
[10] Yatsenko N A 1978 *Thesis of Candidate of Science* Moscow Physical-Technical Institute in Russian
[11] Yatsenko N A 1988 *Preprint* IPM AN SSSR No 338, Moscow in Russian
[12] Kirchner F 1925 *Ann. Phys., Lpz.* 77 287, 298
[13] Githens S 1940 *Phys. Rev.* **57** 822
[14] Chenot M 1948 *Ann. Phys., Paris* **3** 277
[15] Hale D H 1948 *Phys. Rev.* **73** 1046
[16] Pim J A 1949 *Proc. IEE* P III **96** 117
[17] Kihara T 1952 *Rev. Mod. Phys.* **24** 45
[18] Sen S N and Ghosh A K 1962 *Indian J. Phys.* **36** 605
[19] Anashkin G A 1987 *Radiotek. Electron. (Radio Eng. Electron.)* **32** 2567 in Russian
[20] Levitskii S M 1957 *Zh. Tekhn. Fiz.* **27** 970 in Russian
[21] Kropotov N Yu, Kachanov Yu A, Reuka A G, Lisovsky V A, Yegorenkov V D and Farenik V I 1988 *Pis'ma Zh. Tekhn. Fiz.* **14** 359 in Russian
[22] Kirchner F 1947 *Phys. Rev.* **72** 348
[23] Varela A A 1947 *Phys. Rev.* **71** 124
[24] Sen S N and Bhattacharjee B 1965 *Can. J. Phys.* **43** 1543
[25] Sen S N and Bhattacharjee B 1966 *Can. J. Phys.* **44** 3270
[26] Lisovsky V A and Yegorenkov V D 1992 *Pis'ma Zh. Tekhn. Fiz.* **14** 18 66 in Russian
[27] Stalder K R, Anderson C A, Mullan A A and Grahun W G 1992 *J. Appl. Phys.* **72** 1290
[28] Karulina E V and Lebedev Yu A 1988 *J. Phys. D: Appl. Phys.* **21** 411
[29] Sá P A, Loureiro J and Ferreira C M 1992 *J. Phys. D: Appl. Phys.* **25** 960
[30] Kaganovich I D and Tsendin L D 1992 *IEEE Trans. Plasma Sci.* **20** 66
[31] Kropotov N Yu, Lisovsky V A and Farenik V I 1989 *Materialy II Vsesoyuznogo Soveshchaniya po vysokochastotnomy razryadu v volnovykh polyakh (Proc. II All Union Meeting on RF discharge in wave fields) (Kuibyshev)* p 11
[32] Lisovsky V and Yegorenkov V 1993 *Book of Abstracts 9th Int. Conf. on Thin Films (Vienna)* p 99
[33] Raizer Yu P 1987 *Fizika Gazovogo Razryada (Gas Discharge Physics)* (Moscow: Nauka) in Russian
[34] Schlumbohm H 1959 *Z. Ang. Phys.* **11** 156
[35] von Engel A 1955 *Ionized Gases* (Oxford: Clarendon)
[36] Francis G 1960 *Ionization Phenomena in Gases* (London: Butterworths)
[37] Meek J M and Craggs J D 1953 *Electrical Breakdown of Gases* (Oxford: Clarendon)
[38] Fricke H 1933 *Z. Phys.* **86** 464
[39] Meyer E 1919 *Ann. Phys.* **58** 297
[40] Meyer E 1921 *Ann. Phys.* **65** 335
[41] Varnerin L J and Brown S C 1950 *Phys. Rev.* **79** 946
[42] Brown S C 1951 *Proc. IRE* **39** 1493